Journal of Advanced Research in Numerical Heat Transfer

Journal homepage:
https://semarakilmu.com.my/journals/index.php/arnht/index
ISSN: 2735-0142

Heat Transfer Optimization using RSM for Hybrid Nanofluid Flow Impinging Obliquely on a Permeable Shrinking Sheet

Rusya Iryanti Yahaya[1,*], Mohd Shafie Mustafa[2], Norihan Md Arifin[1,2], Ioan Pop[3], Fadzilah Md Ali[1,2], Siti Suzilliana Putri Mohamed Isa[1,4]

[1] Institute for Mathematical Research, Universiti Putra Malaysia, 43400 Serdang, Selangor, Malaysia
[2] Department of Mathematics and Statistics, Faculty of Science, Universiti Putra Malaysia, 43400 Serdang, Selangor, Malaysia
[3] Department of Mathematics, Babeş-Bolyai University, 400084 Cluj-Napoca, Romania
[4] Centre of Foundation Studies for Agricultural Science, Universiti Putra Malaysia, 43400 Serdang, Selangor, Malaysia

ARTICLE INFO

Article history:
Received 10 October 2024
Received in revised form 12 November 2024
Accepted 16 December 2024
Available online 30 January 2025

Keywords:
Hybrid nanofluid; Oblique stagnation-point flow; RSM; Suction; Stability analysis

ABSTRACT

Fluid flow may strike a surface at an angle due to the physical limitations of the nozzle or contouring of the surface. The heat transfer optimization for the Al_2O_3-Cu/water hybrid nanofluid flow impinging obliquely on a permeable shrinking sheet is analyzed in this study. Flow over a shrinking sheet may occur during polymer and metal sheet extraction, wire drawing, and glass-fiber production. The first step in this study involves reducing the governing partial differential equations and boundary conditions into non-linear ordinary differential equations via similarity transformation. Subsequently, these equations are solved using built-in finite difference code in MATLAB bvp4c solver. It is found that the increment of the suction parameter enhances the heat transfer rate represented by the physical quantity of interest called the local Nusselt number. However, the opposite occurs when the nanoparticle volume fraction of Cu and the magnitude of the shrinking parameter increase. Meanwhile, the normal and shear components of skin friction are augmented by the rise in the suction parameter and nanoparticle volume fraction of Cu. Then, the statistical analysis and optimization done using the response surface methodology (RSM) revealed that the local Nusselt number ($Re_x^{-1/2}Nu_x$) is highly impacted by the suction parameter (S), followed by the shrinking parameter (λ) and nanoparticle volume fraction of Cu (ϕ_{Cu}). The maximum value of $Re_x^{-1/2}Nu_x$ is approximated to be 13.30539 when the magnitude of S is at the highest, while $|\lambda|$ and ϕ_{Cu} are at the lowest (i.e., $S = 2.2$, $\lambda = -0.8$, and $\phi_{Cu} = 0.01$).

1. Introduction

A hybrid nanofluid is a heat transfer fluid containing two different nanoparticles suspended in a conventional fluid, such as engine oil, ethylene glycol, water, and blood. Hybrid nanofluids' thermophysical properties and flow behavior have been actively investigated due to their abundant potential applications in various fields and industries. For example, the magnetohydrodynamics (MHD) flow of hybrid nanofluid over a flat elastic surface used in the solar collector was analyzed by

* *Corresponding author.*
E-mail address: rusyairyanti@gmail.com

https://doi.org/10.37934/arnht.29.1.115

Bhatti *et al.,* [1] and Bhatti *et al.,* [2]. Then, Jalili *et al.,* [3] examined hybrid nanofluid's application for drug delivery through an oblique artery with minor stenosis. An extensive investigation on the utilization of hybrid nanofluid in machining was conducted by Kursus *et al.,* [4]. Other applications of hybrid nanofluids include the automobile industry, heat pumps, generators, radioactive systems, and biotechnology [5]. Meanwhile, boundary layer hybrid nanofluid flow over moving surfaces may occur during plastic extrusion, plate, paper, and glass-fiber production. Thus, researchers scrutinized the hybrid nanofluid flow over various stretching surfaces with different flow conditions (see [6-14]). The flow and heat transfer analyses were done by interpreting the solutions of the governing boundary value problem. Meanwhile, several researchers have also examined the hybrid nanofluid flow past shrinking surfaces (see [15-18]). In these studies, suction was applied in the boundary to maintain a steady flow over the shrinking surface [19]. Dual solutions were produced while solving the boundary value problem of these studies, and only one solution was stable in the stability analysis.

Stagnation-point flow occurs when fluid flow impinges orthogonally on a solid surface and separates about a point called the stagnation point. The stagnation point is characterized by zero fluid velocity and maximum mass and heat transfers [20]. There are varieties of applications for stagnation-point flow, including for aerodynamic industries, cooling of electronic devices and nuclear reactors, wire drawing, and plastic extrusion [21]. When a fluid flow strikes a solid surface obliquely, the flow is known as the oblique stagnation-point flow, which consists of the orthogonal stagnation-point flow and a shear flow with a specified vorticity at infinity. Reza and Gupta [22] analyzed the oblique stagnation-point flow of viscous fluid past a stretching surface. As the stretching velocity exceeded the velocity of the surrounding fluid, the flow produced an inverted boundary layer structure. The surface shear stress was then found to decrease as the free stream velocity increased. Then, Tooke and Blyth [23] introduced a free parameter representing the horizontal pressure gradient related to the shear flow. A reversed flow region was observed near the solid boundary due to the significant adverse pressure gradient. Meanwhile, Mahapatra *et al.,* [24] examined the flow over a shrinking sheet with thermal radiation. Compared to the stretching sheet, the similarity solution for the shrinking sheet may or may not exist and may be unique or non-unique depending on the shrinking and free stream velocities ratio. Additionally, a reverse flow was observed in the vicinity of the sheet. Rahman *et al.,* [25] then studied the effects of strain rate, Brownian motion, and thermophoresis towards the oblique stagnation-point flow of nanofluid over a shrinking sheet. The increment of strain rate was observed to enhance the flow's obliquity and shift the dividing streamlines' position away from the stagnation point. Later, Yahaya *et al.,* [26] considered the oblique stagnation-point flow of a hybrid nanofluid past a shrinking sheet. A reduction in the shear component of skin friction was observed due to the increase in the free parameter. This study was then extended by Yahaya *et al.,* [27] to the case of a permeable shrinking sheet with suction. Shear and normal components of skin friction, as well as the temperature gradient, were all amplified by the suction parameter.

In the current study, the work of Yahaya *et al.,* [27] is further extended by incorporating the response surface methodology (RSM). RSM is a statistical tool used to analyze the interactive impacts of parameters on response and predict the optimal conditions for response. Various research has included the RSM in analyzing fluids' flow and thermal behaviors. For example, Neethu *et al.,* [28] examined the electromagnetohydrodynamic hybrid nanofluid flow over a stretching sheet with stratification. The RSM was utilized to find the condition that maximizes the drag coefficient. The desired condition was obtained when the Hartmann number and electric field parameter were at the lowest and the highest values, respectively. Meanwhile, Panda *et al.,* [29] applied the RSM to analyze the heat transfer rate between a hybrid nanofluid and a shrinking/stretching sheet embedded in a porous medium. Through the RSM, Khashi'ie *et al.,* [30] found that the local Nusselt number and skin

friction coefficient in the mixed convection hybrid nanofluid flow over a vertical wedge were greatly influenced by the volumetric concentration of nanoparticle and wedge factor. Yahaya *et al.,* [31] also included the RSM in studying the hybrid nanofluid flow with radiation effect over a biaxial shrinking/stretching surface.

In line with prior research, the RSM will also be used in the current work to find the optimum condition for heat transfer in hybrid nanofluid oblique stagnation-point flow over a permeable shrinking sheet. The RSM was neglected in the prior study by Yahaya *et al.,* [27]. Subsequently, the current study will utilize the RSM to provide further insights into the interactive effects of certain parameters on the local Nusselt number, their significance, and optimal settings. The current flow problem will be represented mathematically as partial differential equations. Then, the flow and thermal behaviors are analyzed based on the numerical findings from the MATLAB bvp4c solver. Lastly, the RSM will investigate the correlation between controlling parameters and the local Nusselt number. All results will be analyzed and discussed.

2. Problem Formulation

The mathematical formulation and configuration of the current steady flow problem follow the study conducted by Yahaya *et al.,* [27]:

$$\frac{\partial u}{\partial x}+\frac{\partial v}{\partial y}=0, \tag{1}$$

$$u\frac{\partial u}{\partial x}+v\frac{\partial u}{\partial y}=-\frac{1}{\rho_{hnf}}\left[\frac{\partial p}{\partial x}+\mu_{hnf}\left(\frac{\partial^2 u}{\partial x^2}+\frac{\partial^2 u}{\partial y^2}\right)\right], \tag{2}$$

$$u\frac{\partial v}{\partial x}+v\frac{\partial v}{\partial y}=-\frac{1}{\rho_{hnf}}\left[\frac{\partial p}{\partial y}+\mu_{hnf}\left(\frac{\partial^2 v}{\partial x^2}+\frac{\partial^2 v}{\partial y^2}\right)\right], \tag{3}$$

$$u\frac{\partial T}{\partial x}+v\frac{\partial T}{\partial y}=\frac{k_{hnf}}{\left(\rho\, C_p\right)_{hnf}}\left(\frac{\partial^2 T}{\partial x^2}+\frac{\partial^2 T}{\partial y^2}\right), \tag{4}$$

$$\left.\begin{array}{l} u=ax, \quad v=v_w, \quad T=T_w \quad \text{at} \quad y=0, \\ u=bx+cy, \quad v=-by, \quad T=T_\infty \quad \text{as} \quad y\to\infty. \end{array}\right\}. \tag{5}$$

The hybrid nanofluid's density (ρ_{Hnf}), dynamic viscosity (μ_{Hnf}), thermal conductivity (k_{Hnf}), and heat capacity $\left(\left(\rho C_p\right)_{Hnf}\right)$ have the correlations given in Table 1 with Bf and ϕ as the base fluid and nanoparticle volume fraction, respectively.

Table 1
Thermophysical properties of hybrid nanofluid [32]

Properties	Correlation
Dynamic viscosity	$\mu_{Hnf} = \frac{\mu_{Bf}}{\left(1-\phi_{Al_2O_3}-\phi_{Cu}\right)^{2.5}}$
Density	$\rho_{hnf} = \left(1-\phi_{Al_2O_3}-\phi_{Cu}\right)\rho_{Bf} + \phi_{Al_2O_3}\rho_{Al_2O_3} + \phi_{Cu}\rho_{Cu}$
Thermal conductivity	$k_{Hnf} = k_{Bf}\left[\frac{\frac{\phi_{Al_2O_3}k_{Al_2O_3}+\phi_{Cu}k_{Cu}}{\phi_{Al_2O_3}+\phi_{Cu}} + 2k_{Bf} - 2\left(\phi_{Al_2O_3}+\phi_{Cu}\right)\left(k_{Bf} - \frac{\phi_{Al_2O_3}k_{Al_2O_3}+\phi_{Cu}k_{Cu}}{\phi_{Al_2O_3}+\phi_{Cu}}\right)k_f}{\frac{\phi_{Al_2O_3}k_{Al_2O_3}+\phi_{Cu}k_{Cu}}{\phi_{Al_2O_3}+\phi_{Cu}} + 2k_{Bf} + \left(\phi_{Al_2O_3}+\phi_{Cu}\right)\left(k_{Bf} - \frac{\phi_{Al_2O_3}k_{Al_2O_3}+\phi_{Cu}k_{Cu}}{\phi_{Al_2O_3}+\phi_{Cu}}\right)k_f}\right]$
Heat capacity	$(\rho C_p)_{Hnf} = \left(1-\phi_{Al_2O_3}-\phi_{Cu}\right)\left(\rho C_p\right)_{Bf} + \phi_{Al_2O_3}(\rho C_p)_{Al_2O_3} + \phi_{Cu}(\rho C_p)_{Cu}$

Figure 1 shows that the region parallel and perpendicular to the sheet are represented by the Cartesian coordinates of x and y, along with velocity components u and v, respectively. Meanwhile, a, b and c are constants, T is the temperature with subscripts ∞ and w denoting the free stream and surface temperatures, and v_w is the mass transfer velocity with $v_w < 0$ for suction.

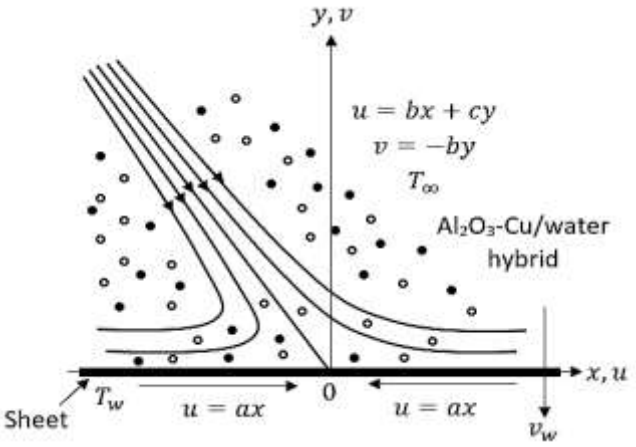

Fig. 1. Fluid flow configuration

In the current study, Al_2O_3-Cu/water hybrid nanofluid is selected as the working fluid due to the desirable features of both nanoparticles and base fluid: water has widespread availability, Al_2O_3 nanoparticles have good chemical inertness, and Cu nanoparticles have high thermal conductivity (see Table 2).

Table 2
Thermophysical properties of Al_2O_3, Cu, and water (H_2O) [33]

Physical properties	H_2O (Bf)	Cu	Al_2O_3
ρ (kg/m^3)	997.1	8933	3970
C_p (J/kg K)	4179	385	765
k (W/m K)	0.613	400	40

Next, the partial differential equations in (2) to (5) will be reduced into non-linear ordinary differential equations using the following similarity variables [27]:

$$\psi = \sqrt{b\,\nu_{Bf}}\,x\,f(\eta) + \frac{c\,\nu_{Bf}}{b}\int_0^{\eta} g(\eta)d\eta,\ \ \theta(\eta) = \frac{T - T_\infty}{T_w - T_\infty},\ \ \eta = y\sqrt{\frac{b}{\nu_{Bf}}}, \tag{6}$$

where ψ is the stream function and ν_{Bf} is the kinematic viscosity. Thus, substituting (6) into Eqs. (2) to (4) results with the following equations:

$$C_1 f^{iv} + f f''' - f'f'' = 0, \tag{7}$$

$$C_1 g''' + f g'' - f''g = 0, \tag{8}$$

$$C_2 \theta'' + Prf \theta' = 0, \tag{9}$$

$$\left.\begin{matrix} f(0) = S, \quad f'(0) = \lambda, \quad g(0) = 0, \quad \theta(0) = 1, \\ f'(\infty) \to 1, \quad g'(\infty) \to 1, \quad \theta(\infty) \to 0, \end{matrix}\right\}, \tag{10}$$

where $C_1 = \frac{\mu_{Hnf}/\mu_{Bf}}{\rho_{Hnf}/\rho_{Bf}}$, $C_2 = \frac{k_{Hnf}/k_{Bf}}{(\rho\, C_p)_{Hnf}/(\rho C_p)_{Bf}}$, $S = -\frac{v_w}{\sqrt{b\, \nu_{Bf}}}$ is the suction parameter, and $\lambda = \left(\frac{a}{b}\right) < 0$ is the shrinking parameter. By utilizing the free stream conditions ($\eta \to \infty$) in (10), and $f(\eta) \sim \eta - \alpha$ and $g(\eta) \sim \eta - \beta$, we integrate Eqs. (7) and (8) with respect to η to form [27]:

$$C_1 f''' + f f'' + 1 - f'^2 = 0, \tag{11}$$

$$C_1 g'' + f g' - f'g + \alpha - \beta = 0, \tag{12}$$

with α and β as constants.

Then,

$$Re_x^{-1/2} Nu_x = -\frac{k_{Hnf}}{k_{Bf}} \theta'(0), \qquad Re_x C_{fx} = \frac{\mu_{Hnf}}{\mu_{Bf}} \left[\xi f''(0) + \frac{c}{b} g'(0)\right], \tag{13}$$

are the local Nusselt number and skin friction coefficient, respectively. Here, $Re_x = \frac{bx^2}{\nu_{Bf}} = \xi^2$ is the local Reynolds number, $f''(0)$ is the normal component of skin friction, and $g'(0)$ is the shear component of skin friction. Meanwhile, the streamlines can be plotted using [27]:

$$\frac{\psi}{\nu_{Bf}} = \xi\, f(\eta) + \frac{c}{b} \int_0^{\eta} g(\eta) d\, \eta, \tag{14}$$

with $\frac{\psi}{\nu_{Bf}} = 0$ denotes the streamline that touches the sheet surface at $\eta = 0$.

3. Heat Transfer Optimization using RSM

It is interesting to analyze the relationship and interactive impacts of three different parameters, specifically, the suction parameter (S), shrinking parameter (λ), and nanoparticle volume fraction of Cu (ϕ_{Cu}), on $Re_x^{-1/2} Nu_x$. Accordingly, the response surface methodology (RSM) will be employed. The three parameters will be denoted as independent variables (X) and $Re_x^{-1/2} Nu_x$ as the response (Res) with a correlation of [34]:

$$Res = c_0 + \sum_{i=1}^{N} c_i X_i + \sum_{i=1}^{N} c_{ii} X_i^2 + \sum_{i=1}^{N-1} \sum_{j=i+1}^{N} c_{ij} X_i X_j \,, \tag{15}$$

where N is the number of independent variables and c is the coefficient. Box and Wilson [35] had pioneered the usage of central composite design for fitting the quadratic model.

In the first step, the independent variables of S, λ, and ϕ_{Cu} are assigned with symbols A, B, and C, respectively. A defined range of actual values is then established for each variable. Subsequently, these actual values are coded into three levels, as shown in Table 3.

Table 3
Independent variables with their actual and coded values

Independent variables	Symbol	Level		
		Low (-1)	Medium (0)	High (1)
S	A	1.8	2.0	2.2
λ	B	-1.4	-1.1	-0.8
ϕ_{Cu}	C	0.01	0.02	0.03

Then, the quadratic model for the current flow problem can be written as:

$$Res = c_0 + c_1\mathrm{A} + c_2\mathrm{B} + c_3\mathrm{C} + c_{11}\mathrm{AA} + c_{22}\mathrm{BB} + c_{33}\mathrm{CC} + c_{12}\mathrm{AB} + c_{13}\mathrm{AC} + c_{23}\mathrm{BC}, \tag{16}$$

where A, B, and C are the coded values. Next, the current study's numerical experiment is based on the face-centered central composite design (FCD). The formula $2^N + 2N + C^*$, with $C^* = 6$ as the center point, yields 20 runs that are appropriate for the selected experimental design. Table 4 tabulates the coded levels and their respective responses for each run.

Table 4
Response values

Runs	Actual values			Coded values			Response
	S	λ	ϕ_{Cu}	A	B	C	
1	1.8	-1.4	0.01	-1	-1	-1	10.45533
2	2.2	-1.4	0.01	1	-1	-1	13.03356
3	1.8	-0.8	0.01	-1	1	-1	10.80052
4	2.2	-0.8	0.01	1	1	-1	13.30618
5	1.8	-1.4	0.03	-1	-1	1	10.41660
6	2.2	-1.4	0.03	1	-1	1	12.98421
7	1.8	-0.8	0.03	-1	1	1	10.77024
8	2.2	-0.8	0.03	1	1	1	13.26460
9	1.8	-1.1	0.02	-1	0	0	10.61704
10	2.2	-1.1	0.02	1	0	0	13.15042
11	2.0	-1.4	0.02	0	-1	0	11.72828
12	2.0	-0.8	0.02	0	1	0	12.03690
13	2.0	-1.1	0.01	0	0	-1	11.90731
14	2.0	-1.1	0.03	0	0	1	11.86718
15	2.0	-1.1	0.02	0	0	0	11.88716
16	2.0	-1.1	0.02	0	0	0	11.88716
17	2.0	-1.1	0.02	0	0	0	11.88716
18	2.0	-1.1	0.02	0	0	0	11.88716
19	2.0	-1.1	0.02	0	0	0	11.88716
20	2.0	-1.1	0.02	0	0	0	11.88716

The third step involves validating the quadratic model (16) by conducting an analysis of variance (ANOVA). The p-value, generated from the ANOVA, helps to identify the significant and insignificant terms. Any insignificant terms with a p-value greater than 0.05 can be eliminated from (16). A new quadratic model equation containing only significant terms and their coefficients is obtained upon eliminating the insignificant term. The impacts of these terms on the response can then be analyzed through the model equation and also from the contour and surface plots.

Finally, the optimization steps are carried out with the aim of maximizing the response. In most studies involving heat transfer analysis, a maximum heat transfer rate is desired for an efficient performance in heating or cooling processes. The heat transfer rate is represented by $Re_x^{-1/2}Nu_x$, which is subsequently referred to as the response. Optimal settings of independent variables that generate the maximum response can be achieved through the utilization of RSM. Thus, it provides excellent information and suggestions for future related work and real-life applications.

4. Results and Discussion

4.1 Analysis of Fluid Flow and Heat Transfer

MATLAB bvp4c solver is employed to numerically solve the boundary value problems (10) to (12). Equation (11) is solved subject to the boundary condition (10) to determine the values of α for different $\phi_{Al_2O_3}$, ϕ_{Cu}, S, and λ. The obtained results undergo comparison with the findings from previous studies that were also computed using MATLAB bvp4c solver. As observed from Table 5, the results are in good agreement; thus, it provides confidence that the current numerical procedure and subsequent numerical results are correct.

Table 5
Results of α for different values of $\phi_{Al_2O_3}$, ϕ_{Cu}, S, and λ

$\phi_{Al_2O_3}$	ϕ_{Cu}	S	λ	α		
				Present study	Yahaya *et al.,* [27]	Rahman *et al.,* [36]
0	0	0	0	0.64790	0.647900	0.6479004
				[-]	[-]	[-]
			-0.8	1.55129	1.551291	1.5512911
				[-]	[-]	[-]
			-1.0	1.96613	1.966129	1.9661288
				[-]	[-]	[-]
0.05	0.05	0	-1.1	2.08540	2.085357	-
				[7.01526]	[7.019518]	[-]

*[ ]: Second solution

Next, the physical quantities of interest for various values of $\phi_{Al_2O_3}$, ϕ_{Cu}, S, and λ are tabulated in Table 6. Dual solutions are found at certain values of the controlling parameters. Following the stability analysis conducted in previous studies, the first solution is physically meaningful for application (see [26] and [27]). The current study will present all solutions to the boundary value problem (10) to (12); however, the discussion will only focus on the behavior of the stable first solution. As observed from Table 6, the addition of ϕ_{Cu} is found to enhance $f''(0)$ and $g'(0)$. At the same time, the value of $Re_x^{-1/2}Nu_x$ diminishes with the increase in ϕ_{Cu}. Interestingly, Yahaya *et al.,* [26] found that the augmentation of ϕ_{Cu} improved the thermal conductivity of the hybrid nanofluid (k_{Hnf}) and raised the local Nusselt number. However, the contrasting behavior observed in the current study may be due to the presence of suction. Nevertheless, increasing the suction parameter improves the physical quantities of interest, comprising the local Nusselt number, shear, and normal

components of skin friction. Meanwhile, $f''(0)$ and $g'(0)$ exhibit dissimilar impacts to the increasing magnitude of the shrinking parameter ($|\lambda|$). The value of $f''(0)$ increases with $|\lambda|$, but the opposite occurs for $g'(0)$. Besides that, the increment of $|\lambda|$ reduces the available surface for heat transfer, lowers the heat transfer rate, and reduces the value of $Re_x^{-1/2}Nu_x$.

Meanwhile, the effects of the nanoparticle volume fraction of Cu on the velocity and temperature profiles of the hybrid nanofluid are presented in Figure 2. As observed from Figures 2a and 2b, the profiles of normal ($f'(\eta)$) and shear ($g(\eta)$) flow velocities are enhanced by the augmentation of ϕ_{Cu}. Meanwhile, the momentum boundary layers diminish as ϕ_{Cu} increases. In Figure 2c, the temperature profile is seen to rise with ϕ_{Cu}. The increment of ϕ_{Cu} augments k_{Hnf} and improves the heat transmission from the sheet to the hybrid nanofluid. The temperature profile rises, the thermal boundary layer thickens, and the temperature gradient drops. However, it is noted from Table 6 that the local Nusselt number reduces as ϕ_{Cu} increases. Hence, it denotes that the temperature gradient term ($-\theta'(0)$) exceeds the thermal conductivity term $\left(\frac{k_{Hnf}}{k_{Bf}}\right)$ in influencing the local Nusselt number $\left(Re_x^{-1/2}Nu_x = -\frac{k_{Hnf}}{k_{Bf}}\theta'(0)\right)$ and heat transfer rate.

Table 6
Physical quantities of interest for various values of $\phi_{Al_2O_3}$, ϕ_{Cu}, S, and λ when $Pr = 6.2$ and $\alpha = \beta$

$\phi_{Al_2O_3}$	ϕ_{Cu}	S	λ	$f''(0)$	$g'(0)$	$Re_x^{-1/2}Nu_x$
0.02	0.01	2	-1.1	5.08541	4.91529	11.90731
				[-1.50917]	[-0.08080]	[0.06855]
	0.02	1.8		4.85581	4.23916	10.61704
				[-1.21172]	[-0.04285]	[0.00235]
		2	-0.8	4.72414	5.36332	12.03690
				[-1.85109]	[-0.04534]	[0.02407]
			-1.1	5.28001	5.09938	11.88716
				[-1.63436]	[-0.09375]	[0.19039]
			-1.4	5.44645	5.00893	11.83531
				[-1.55250]	[-0.12029]	[0.36209]
		2.2	-1.1	5.70752	6.04442	13.15042
				[-2.13664]	[-0.17936]	[4.61305]
	0.03	2	-1.1	5.46006	5.26976	11.86718
				[-1.75441]	[-0.10680]	[0.41504]

*[ ]: Second solution

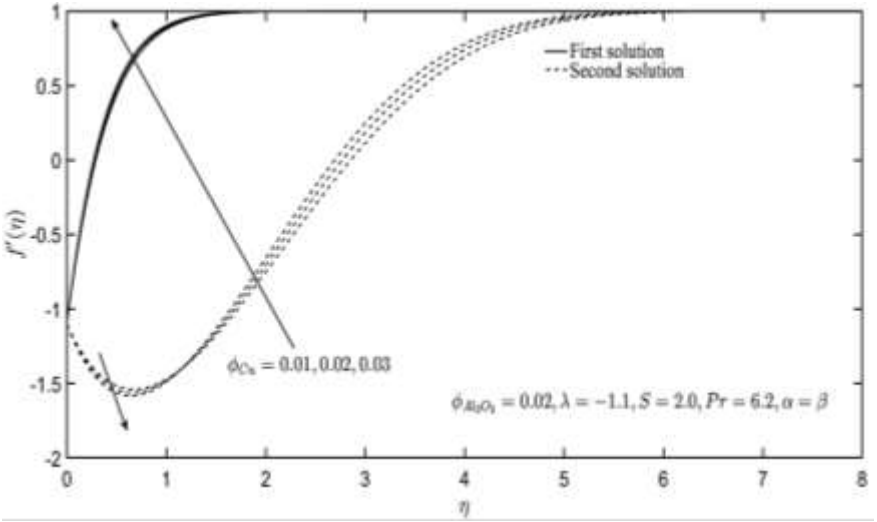

(a)

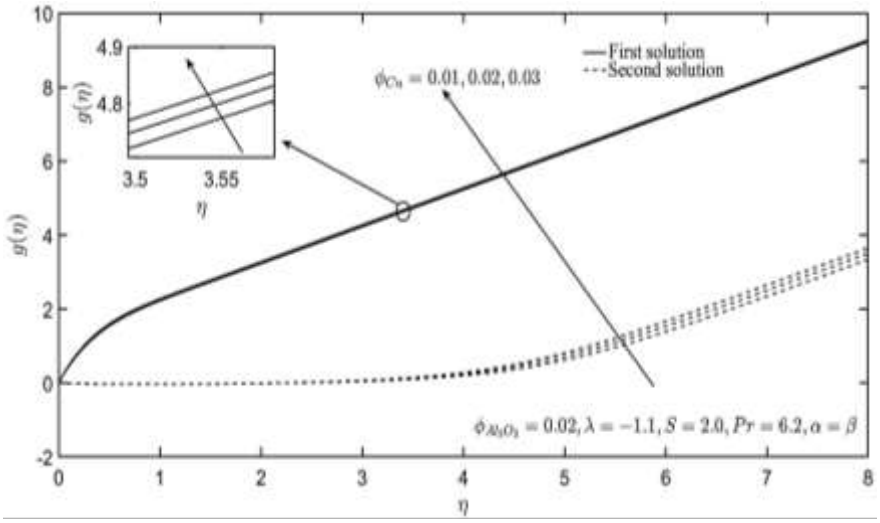

(b)

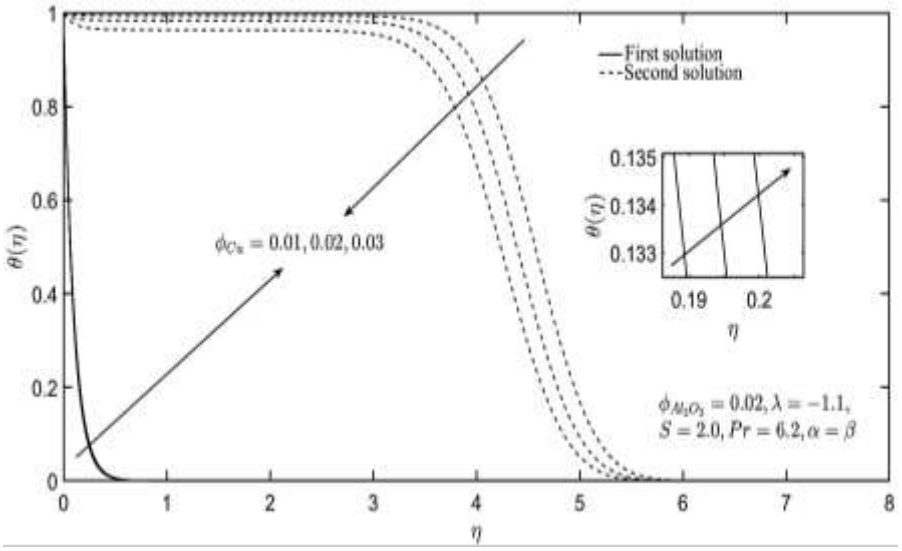

(c)

Fig. 2. Effects of ϕ_{Cu} towards the velocity and temperature profiles

Figures 3a and 3b then depict the decreasing profiles of normal and shear flow velocities with the increasing magnitude of the shrinking parameter ($|\lambda|$). Based on Figure 3a, the hybrid nanofluid flow experiences a notable reduction in velocity near the shrinking sheet. After a certain value of η (i.e., some distance from the sheet), the shrinking of the sheet has less impact on the flow. Eventually, the fluid attains free stream velocity. The reduction of flow velocity by the increment in $|\lambda|$ then enlarges the momentum boundary layer thickness (see Figure 3a). Meanwhile, Figure 3c shows that the temperature profile and thermal boundary layer thickness increase with $|\lambda|$.

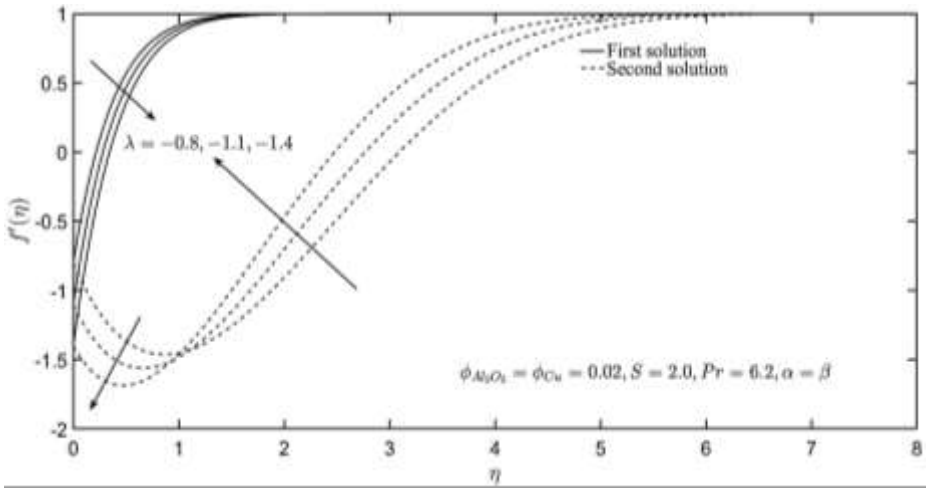

(a)

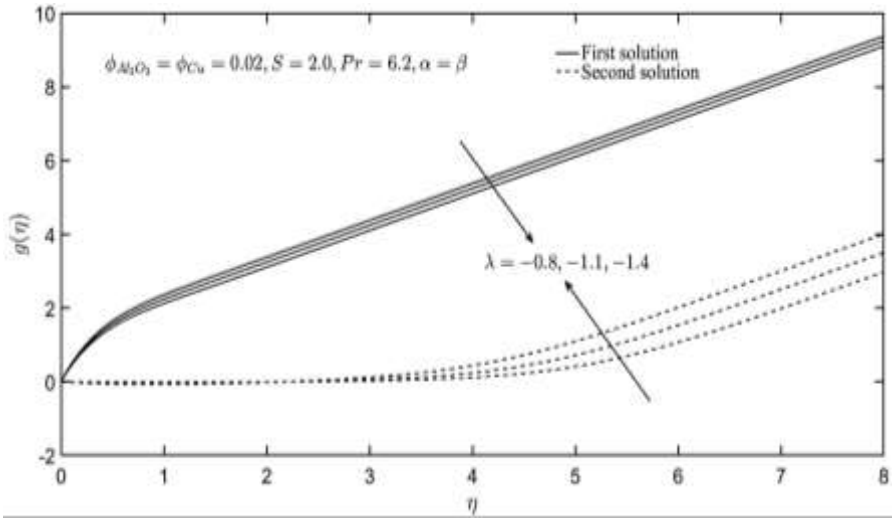

(b)

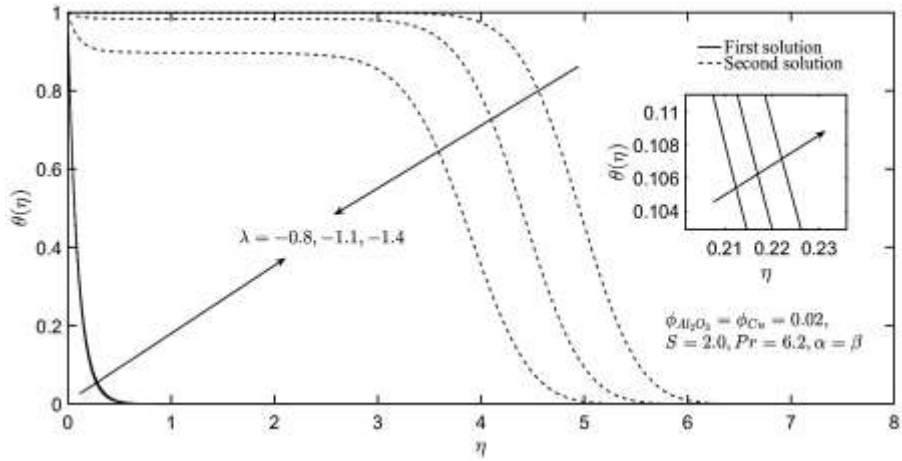

(c)

Fig. 3. Effects of λ towards the velocity and temperature profiles

4.2 Statistical Investigation

Following the third step of RSM discussed in the previous section, the ANOVA is conducted in Table 7. Based on this table, the term CC is found to have a p-value of 0.953 (> 0.05); thus, the term is insignificant and can be eliminated from correlation (16). The new quadratic model can be written as:

$$Res = 11.8872 + 1.26792\mathrm{A} + 0.156046\mathrm{B} - 0.020007\mathrm{C} - 0.003568\mathrm{AA} - 0.004708\mathrm{BB} - 0.018227\mathrm{AB} - 0.002740\mathrm{AC} + 0.002027\mathrm{BC}, \quad (17)$$

where A, B, and C are the coded values.

Table 7
Results of ANOVA

Source	Degrees of freedom	Adjusted sum of squares	Adjusted mean square	F-value	p-value
Model	9	16.3268	1.8141	1583285.19	0.000
Linear	3	16.3238	5.4413	4748975.18	0.000
A	1	16.0763	16.0763	14030909.65	0.000
B	1	0.2435	0.2435	212522.38	0.000
C	1	0.0040	0.0040	3493.52	0.000
Square	3	0.0003	0.0001	80.09	0.000
AA	1	0.0000	0.0000	30.31	0.000
BB	1	0.0001	0.0001	52.88	0.000
CC	1	0.0000	0.0000	0.00	0.953
2-way interaction	3	0.0028	0.0009	800.29	0.000
AB	1	0.0027	0.0027	2319.76	0.000
AC	1	0.0001	0.0001	52.42	0.000
BC	1	0.0000	0.0000	28.70	0.000
Error	10	0.0000	0.0000		
Lack-of-fit	5	0.0000	0.0000	*	*
Pure error	5	0.0000	0.0000		
Total	19	16.3269			

Then, the interactive impacts of the independent variables are presented in Figure 4. The independent variable A, which symbolizes the suction parameter, is observed to have a superior effect on the response when interacting with variables B (λ) and C (ϕ_{Cu}). The highest response value is obtained at a high level of A (i.e., a coded value of 1). Meanwhile, in the interaction between B and C, the controlling variable B is more dominant than C in affecting the response. The high level of B is observed to augment the response, while the low level of C produces a slightly higher response than the higher level. Thus, the suction parameter has a dominant effect on $Re_x^{-1/2}Nu_x$, followed by the shrinking parameter and the nanoparticle volume fraction of Cu. A high value of the suction parameter can be imposed to produce a high local Nusselt number. In contrast, the lower magnitude of the shrinking parameter and nanoparticle volume fraction of Cu results in a better magnitude of the local Nusselt number. However, these observed behaviors are only applicable to the current flow problem with a selected range of controlling parameters. The results may vary for other flow problems and conditions.

Finally, the last step of RSM is determining the optimal point, which is presented in Table 8. With a desirability of 99.97%, the optimum (i.e., maximum) response is 13.30539, obtained when A = B = 1 and C = −1. Hence, in the current study, the highest value of suction (i.e., $S = 2.2$) with the smallest magnitude of the shrinking parameter (i.e., $\lambda = -0.8$) and nanoparticle volume fraction of Cu (i.e., $\phi_{Cu} = 0.01$) generate the highest value of the local Nusselt number.

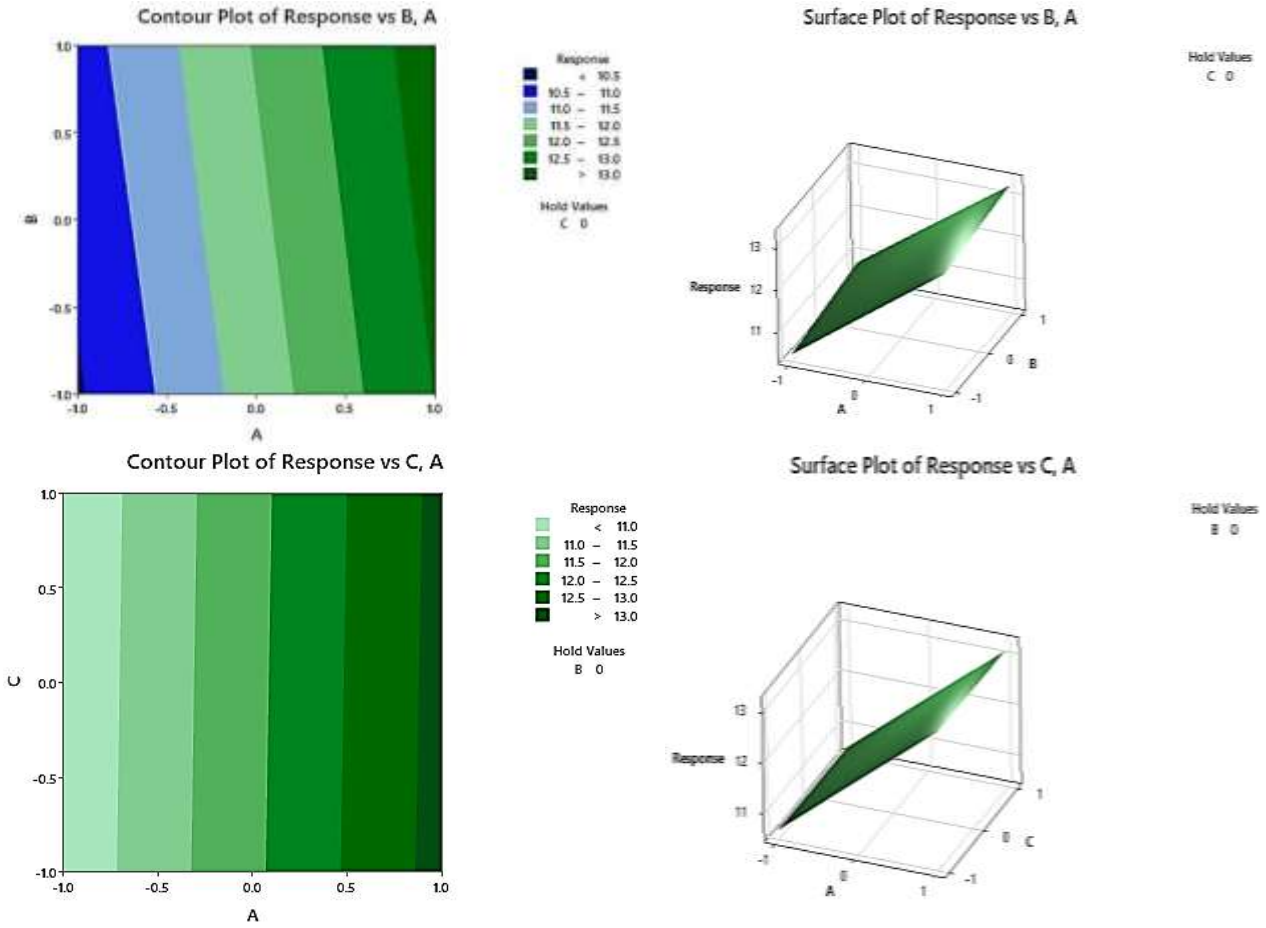

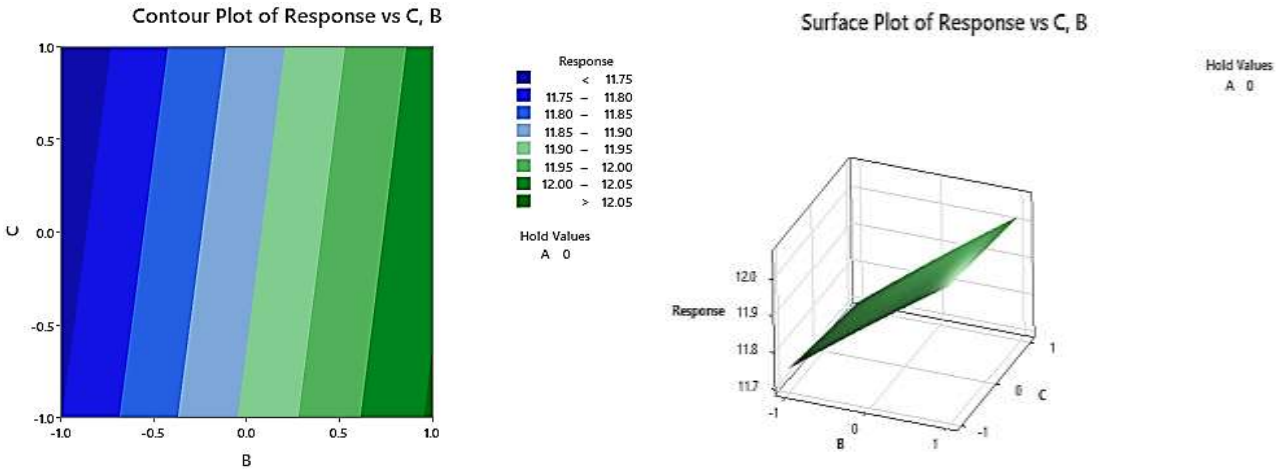

Fig. 4. Surface and contour plots for independent variables and response

Table 8
Optimization

Solution	A	B	C	Response fit	Composite desirability
1	1	1	-1	13.30539	0.999727

5. Conclusion

The steady, two-dimensional, hybrid nanofluid oblique stagnation-point flow over a permeable shrinking sheet is presented mathematically before being solved using MATLAB bvp4c solver. The RSM is utilized to examine the interactive effects of controlling parameters and find the optimal condition for the maximum local Nusselt number. The results are summarized as follows:

i) The value of $Re_x^{-1/2}Nu_x$ diminishes with the rise in $|\lambda|$ and ϕ_{Cu} but increases with the enhancement of S.
ii) The augmentation of ϕ_{Cu} and S increases the values of $f''(0)$ and $g'(0)$.
iii) The increase in $|\lambda|$ enhances and reduces $f''(0)$ and $g'(0)$, respectively.
iv) The local Nusselt number shows a pronounced increase with S, followed by λ and ϕ_{Cu}.
v) The maximum value of $Re_x^{-1/2}Nu_x$ is estimated to be 13.30539 at $S = 2.2$, $\lambda = -0.8$, and $\phi_{Cu} = 0.01$, with a desirability of 99.97%.

Acknowledgement
This research has been funded by the Ministry of Higher Education (MOHE) and Universiti Putra Malaysia through the Fundamental Research Grant Scheme (FRGS) (FRGS/1/2023/STG06/UPM/02/1) and Vote no.:5540632.

References
[1] Bhatti, Muhammad Mubashir, Hakan F. Öztop, and Rahmat Ellahi. "Study of the magnetized hybrid nanofluid flow through a flat elastic surface with applications in solar energy." *Materials* 15, no. 21 (2022): 7507. https://doi.org/10.3390/ma15217507
[2] Bhatti, M. M., Hakan F. Öztop, R. Ellahi, Ioannis E. Sarris, and Mohammad Hossein Doranehgard. "Insight into the investigation of diamond (C) and Silica (SiO2) nanoparticles suspended in water-based hybrid nanofluid with application in solar collector." *Journal of Molecular Liquids* 357 (2022): 119134. https://doi.org/10.1016/j.molliq.2022.119134

[3] Jalili, Payam, Ahmad Sadeghi Ghahare, Bahram Jalili, and Davood Domiri Ganji. "Analytical and numerical investigation of thermal distribution for hybrid nanofluid through an oblique artery with mild stenosis." *SN Applied Sciences* 5, no. 4 (2023): 95. https://doi.org/10.1007/s42452-023-05312-z

[4] Kursus, Maisarah, Pay Jun Liew, Nor Azwadi Che Sidik, and Jingsi Wang. "Recent Progress on the Application of Nanofluids and Hybrid Nanofluids in Machining: A Comprehensive Review. " *The International Journal of Advanced Manufacturing Technology* 121, no. 3–4 (2022): 1455–81. https://doi.org/10.1007/s00170-022-09409-4

[5] Elattar, Samia, Maha M. Helmi, Mohamed Abdelghany Elkotb, M. A. El-Shorbagy, Anas Abdelrahman, Muhammad Bilal, and Aatif Ali. "Computational assessment of hybrid nanofluid flow with the influence of hall current and chemical reaction over a slender stretching surface." *Alexandria Engineering Journal* 61, no. 12 (2022): 10319-10331. https://doi.org/10.1016/j.aej.2022.03.054

[6] Waqas, Hassan, Umar Farooq, Dong Liu, Muhammad Abid, Muhammad Imran, and Taseer Muhammad. "Heat transfer analysis of hybrid nanofluid flow with thermal radiation through a stretching sheet: A comparative study." *International Communications in Heat and Mass Transfer* 138 (2022): 106303. https://doi.org/10.1016/j.icheatmasstransfer.2022.106303

[7] Shah, Syed Asif Ali, N. Ameer Ahammad, ElSayed M. Tag El Din, Fehmi Gamaoun, Aziz Ullah Awan, and Bagh Ali. "Bio-convection effects on prandtl hybrid nanofluid flow with chemical reaction and motile microorganism over a stretching sheet." *Nanomaterials* 12, no. 13 (2022): 2174. https://doi.org/10.3390/nano12132174

[8] Abbas, Nadeem, Khalil Ur Rehman, Wasfi Shatanawi, and M. Y. Malik. "Numerical study of heat transfer in hybrid nanofluid flow over permeable nonlinear stretching curved surface with thermal slip." *International Communications in Heat and Mass Transfer* 135 (2022): 106107. https://doi.org/10.1016/j.icheatmasstransfer.2022.106107

[9] Neethu, T. S., A. S. Sabu, Alphonsa Mathew, A. Wakif, and Sujesh Areekara. "Multiple linear regression on bioconvective MHD hybrid nanofluid flow past an exponential stretching sheet with radiation and dissipation effects." *International Communications in Heat and Mass Transfer* 135 (2022): 106115. https://doi.org/10.1016/j.icheatmasstransfer.2022.106115

[10] Farooq, Umar, Hassan Waqas, Taseer Muhammad, Muhammad Imran, and Ali Saleh Alshomrani. "Computation of nonlinear thermal radiation in magnetized nanofluid flow with entropy generation." *Applied Mathematics and Computation* 423 (2022): 126900. https://doi.org/10.1016/j.amc.2021.126900

[11] Sulochana, C., and Geeta C. Shivapuji. "Numerical analysis of hybrid nanofluid flow over a nonlinear stretching sheet with viscous dissipation, Joule heating effects." CFD Letters 14, no. 10 (2022): 43-55. https://doi.org/10.37934/cfdl.14.10.4255

[12] Abdullah, Nur Nazirah, Ahmad Nazri Mohamad Som, Norihan Md Arifin, and Aniza Ab Ghani. "The Effect of MHD on Marangoni Boundary Layer of Hybrid Nanofluid Flow Past a Permeable Stretching Surface." CFD Letters 15, no. 5 (2023): 65-73. https://doi.org/10.37934/cfdl.15.5.6573

[13] Bilal, Muhammad, Aatif Ali, Hala A. Hejazi, and Samy Refahy Mahmuod. "Numerical study of an electrically conducting hybrid nanofluid over a linearly extended sheet." *ZAMM-Journal of Applied Mathematics and Mechanics/Zeitschrift für Angewandte Mathematik und Mechanik* 103, no. 5 (2023): e202200227. https://doi.org/10.1002/zamm.202200227

[14] Rafique, Khadija, Zafar Mahmood, and Umar Khan. "Mathematical analysis of MHD hybrid nanofluid flow with variable viscosity and slip conditions over a stretching surface." *Materials Today Communications* 36 (2023): 106692. https://doi.org/10.1016/j.mtcomm.2023.106692

[15] Wahid, Nur Syahirah, Norihan Md Arifin, Najiyah Safwa Khashi'ie, and Ioan Pop. "Mixed convection MHD hybrid nanofluid over a shrinking permeable inclined plate with thermal radiation effect." *Alexandria Engineering Journal* 66 (2023): 769-783. https://doi.org/10.1016/j.aej.2022.10.075

[16] Yasir, Muhammad, Masood Khan, A. S. Alqahtani, and M. Y. Malik. "Mass transpiration effect on rotating flow of radiative hybrid nanofluid due to shrinking surface with irregular heat source/sink." *Case Studies in Thermal Engineering* 44 (2023): 102870. https://doi.org/10.1016/j.csite.2023.102870

[17] Asghar, Adnan, Abdul Fattah Chandio, Zahir Shah, Narcisa Vrinceanu, Wejdan Deebani, Meshal Shutaywi, and Liaquat Ali Lund. "Magnetized mixed convection hybrid nanofluid with effect of heat generation/absorption and velocity slip condition." *Heliyon* 9, no. 2 (2023). https://doi.org/10.1016/j.heliyon.2023.e13189

[18] Wahid, Nur Syahirah, Norihan Md Arifin, Najiyah Safwa Khashi'ie, Rusya Iryanti Yahaya, Ioan Pop, Norfifah Bachok, and Mohd Ezad Hafidz Hafidzuddin. "Three-dimensional radiative flow of hybrid nanofluid past a shrinking plate with suction." Journal of Advanced Research in Fluid Mechanics and Thermal Sciences 85, no. 1 (2021): 54-70. https://doi.org/10.37934/arfmts.85.1.5470

[19] Miklavčič, M., and C. Wang. "Viscous flow due to a shrinking sheet." *Quarterly of Applied Mathematics* 64, no. 2 (2006): 283-290.

[20] Zangooee, M. R., Kh Hosseinzadeh, and D. D. Ganji. "Hydrothermal analysis of hybrid nanofluid flow on a vertical plate by considering slip condition." *Theoretical and Applied Mechanics Letters* 12, no. 5 (2022): 100357. https://doi.org/10.1016/j.taml.2022.100357
[21] Sadiq, Muhammad Adil. "MHD stagnation point flow of nanofluid on a plate with anisotropic slip." *Symmetry* 11, no. 2 (2019): 132. https://doi.org/10.3390/sym11020132
[22] Reza, M., and A. S. Gupta. "Steady two-dimensional oblique stagnation-point flow towards a stretching surface." *Fluid Dynamics Research* 37, no. 5 (2005): 334. https://doi.org/10.1016/j.fluiddyn.2005.07.001
[23] Tooke, R. M., and M. G. Blyth. "A note on oblique stagnation-point flow." *Physics of Fluids* 20, no. 3 (2008). https://doi.org/10.1063/1.2876070
[24] Mahapatra, Tapas Ray, Samir Kumar Nandy, and Anadi Sankar Gupta. "Oblique stagnation-point flow and heat transfer towards a shrinking sheet with thermal radiation." *Meccanica* 47 (2012): 1325-1335. https://doi.org/10.1007/s11012-011-9516-z
[25] Rahman, M. M., Teodor Grosan, and Ioan Pop. "Oblique stagnation-point flow of a nanofluid past a shrinking sheet." *International Journal of Numerical Methods for Heat & Fluid Flow* 26, no. 1 (2016): 189-213. https://doi.org/10.1108/HFF-10-2014-0315
[26] Yahaya, Rusya Iryanti, Norihan Md Arifin, Roslinda Mohd Nazar, and Ioan Pop. " Oblique stagnation-point flow past a shrinking surface in a cu-al2o3/h2o hybrid nanofluid." *Sains Malaysiana* 50, no. 10 (2021): 3139-3152. http://doi.org/10.17576/jsm-2021-5010-25
[27] Yahaya, Rusya Iryanti, Norihan Md Arifin, Ioan Pop, Fadzilah Md Ali, and Siti Suzilliana Putri Mohamed Isa. "Dual solutions for the oblique stagnation-point flow of hybrid nanofluid towards a shrinking surface: Effects of suction." *Chinese Journal of Physics* 81 (2023): 193-205. https://doi.org/10.1016/j.cjph.2022.12.004
[28] Neethu, T. S., Sujesh Areekara, A. S. Sabu, Alphonsa Mathew, and K. K. Anakha. "Bioconvective electromagnetohydrodynamic hybrid nanoliquid flow over a stretching sheet with stratification effects: a four-factor response surface optimized model." *Waves in Random and Complex Media* (2022): 1-26. https://doi.org/10.1080/17455030.2022.2066218
[29] Panda, Subhajit, Surender Ontela, S. R. Mishra, and P. K. Pattnaik. "Response surface methodology and sensitive analysis for optimizing heat transfer rate on the 3D hybrid nanofluid flow through permeable stretching surface." *Journal of Thermal Analysis and Calorimetry* 148, no. 14 (2023): 7369-7382. https://doi.org/10.1007/s10973-023-12183-4
[30] Khashi'ie, Najiyah Safwa, Iskandar Waini, Mohd Fariduddin Mukhtar, Nurul Amira Zainal, Khairum Bin Hamzah, Norihan Md Arifin, and Ioan Pop. "Response surface methodology (RSM) on the hybrid nanofluid flow subject to a vertical and permeable wedge." *Nanomaterials* 12, no. 22 (2022): 4016. https://doi.org/10.3390/nano12224016
[31] Yahaya, Rusya Iryanti, Mohd Shafie Mustafa, Norihan Md Arifin, Ioan Pop, Fadzilah Md Ali, and Siti Suzilliana Putri Mohamed Isa. "Hybrid nanofluid flow past a biaxial stretching/shrinking permeable surface with radiation effect: Stability analysis and heat transfer optimization." *Chinese Journal of Physics* 85 (2023): 402-420. https://doi.org/10.1016/j.cjph.2023.06.003
[32] Takabi, Behrouz, and Saeed Salehi. "Augmentation of the heat transfer performance of a sinusoidal corrugated enclosure by employing hybrid nanofluid." *Advances in Mechanical Engineering* 6 (2014): 147059. https://doi.org/10.1155/2014/147059
[33] Jamaludin, Anuar, Nor Ain Azeany Mohd Nasir, Roslinda Nazar, and Ioan Pop. "MHD opposing flow of Cu− TiO2 hybrid nanofluid under an exponentially stretching/shrinking surface embedded in porous media with heat source and slip impacts." *Results in Engineering* 17 (2023): 101005. https://doi.org/10.1016/j.rineng.2023.101005
[34] Mahanthesh, B., K. Thriveni, Puneet Rana, and Taseer Muhammad. "Radiative heat transfer of nanomaterial on a convectively heated circular tube with activation energy and nanoparticle aggregation kinematic effects." *International Communications in Heat and Mass Transfer* 127 (2021): 105568. https://doi.org/10.1016/j.icheatmasstransfer.2021.105568
[35] Box, George EP, and Kenneth B. Wilson. "On the experimental attainment of optimum conditions." In *Breakthroughs in statistics: methodology and distribution*, pp. 270-310. New York, NY: Springer New York, 1992.
[36] Rahman, M. M., Teodor Grosan, and Ioan Pop. "Oblique stagnation-point flow of a nanofluid past a shrinking sheet." *International Journal of Numerical Methods for Heat & Fluid Flow* 26, no. 1 (2016): 189-213. https://doi.org/10.1108/HFF-10-2014-0315